

Structural and electronic properties of aluminum-based binary clusters

S. Chacko,* M. Deshpande,[†] and D. G. Kanhere[‡]

Department of Physics, University of Pune, Pune 411007, India

(Received 2 October 2000; revised manuscript received 5 April 2001; published 1 October 2001)

We investigate the low-energy geometries and the electronic structure of several aluminum based clusters, viz. Al_4X_4 , ($X=Li, Na, K, Be, Mg, B,$ and Si) by first principle Born-Oppenheimer molecular dynamics within the framework of density-functional theory. We present a systematic analysis of the bonding properties and discuss the validity of spherical jellium model. We find that the structure of eigenstates for clusters with metallic elements conform to the spherical jellium model. The 20 valence electron systems Al_4Be_4 and Al_4Mg_4 exhibit a large highest-occupied–lowest-unoccupied (HOMO-LUMO) gap due to shell closing effect. In clusters containing alkali-metal atom, Al_4 behaves as a superatom that is ionically bonded to them. The Al-Al bond in both Al_4Si_4 and Al_4B_4 clusters is found to be covalent.

DOI: 10.1103/PhysRevB.64.155409

PACS number(s): 61.46.+w, 31.15.Ar, 36.40.–c

I. INTRODUCTION

During the last few years much attention has been paid to the study of atomic clusters from both theoretical and experimental^{1–4} sides. The areas of interest include ground-state geometries, electronic structure, optical properties, fragmentation, and thermodynamic properties like melting. The theoretical calculations are usually carried out by employing density-functional molecular dynamics in conjunction with simulated annealing. Extensive investigations on the geometries and the electronic structure of homo-atomic clusters (with ≈ 20 atoms) of Li, Na, K, Mg, B, Al, Ga, Si, etc., have been carried out.^{5–14} Similar investigations on heterogeneous clusters are relatively few. Mixed clusters are of considerable interest due to diverse effects like bonding,^{15,16} segregation, selective clustering, etc. It is instructive to contrast the properties of these tiny alloys with their bulk counterparts. Another interesting aspect concerns the validity of spherical jellium model¹⁷ (SJM) for mixed clusters. It is known that the eigenvalue spectrum of alkali-atom clusters generally conforms to the SJM with minor modifications. This has also been observed in the case of single impurity doped metallic clusters of the type A_nB ,^{18–23} where depending upon the nature of impurity, it either gets trapped or prefers to be on the surface or distorts the host structure significantly. Impurities with smaller ionic radii and strong binding with the host are seen to get trapped in the cluster. Many investigations on mixing and segregation effects in various mixed alkali-atom clusters, viz. Na-K (Refs. 24 and 25) and Na-Li (Ref. 26), have been reported. The ground-state geometries of several A_4B_4 clusters involving simple metal atoms like Li, Na, K, Rb, Cs, Mg, Al, Sb, and other elements like Ga, Sr, Si have been studied by Majumdar *et al.*²⁷ The lowest energy structure of all these clusters were found to be tetracapped tetrahedron (TCP). In an *ab initio* orbital based investigation, Raghavachari *et al.*²⁸ suggested a similar structure for both Al_4P_4 and Mg_4S_4 clusters. A recent *ab initio* density-functional calculation²⁹ demonstrated the high stability of A_4Pb_4 ($A=Li, Na, K, Rb, Cs$) clusters, where Pb_4 forms a tetrahedron capped by alkali atoms.

It is well established that so far as alkali-metal atoms are concerned the SJM has been quite successful in describing

the gross electronic structure and the stability. However, clusters of Al presents an interesting contrast. Although bulk Al is known to be a free electron metal, several experimental and theoretical studies indicate that small Al clusters do not display the well known magic behavior. This and other such issues concerning the nature of the electronic states in pure Al clusters have been critically examined by Rao and Jena.³⁰ In an elaborate density-functional calculations for charged and neutral Al clusters, they found that Al_7^+ with 20 valence electrons is magic. Further, the electronic structure of clusters containing less than 7 atoms does not resemble that of the jellium model. They have also presented some evidence for an effective monovalent nature in pure small Al clusters. However, their investigation on Al_5X_m (Ref. 31) ($X=Li, K$) failed to provide any evidence of suggested monovalent nature of Al. The onset of *sp* hybridization in pure Al clusters and the relation of their electronic structure to the jellium model has also been studied by Duque and Mananes³². Recent investigations on Al_5Na_n (Ref. 33) ($n=1–6$), clearly indicate that Al_5Na_5 , a 20 valence electron system, to be very stable. The spectrum of Al_5Na_5 conforms to SJM. Moreover, alkalization of these Al clusters³¹ makes their electronic structure jelliumlike. It also lowers the ionization potential of the base Al_n clusters.³⁴ Apart from these peculiarities of Al clusters, early work on Al-Li clusters^{18,35} indicates an ionic bond between Al and Li. It may be recalled that in bulk phase, aluminum forms stable alloys with various elements like Li, Be, Mg, Si, etc., while Na and K (Refs. 36 and 37) are completely immiscible in it. It also forms a strongly bonded boride AlB_2 , whose stability mainly depend on the strong B-B and Al-B bond. Thus it is of considerable interest to study aluminum based mixed clusters.

In the present work, we investigate the structural and the electronic properties of several aluminum based binary clusters, viz. Al_4X_4 clusters using Born–Oppenheimer molecular dynamics (BOMD) (Ref. 38) within the framework of density-functional theory, where X ranges from simple monovalent alkali metals (Li, Na, K) to divalent metals (Be, Mg) and finally to semiconductors B and Si. We also present a systematic analysis of the bonding properties and discuss the validity of SJM.

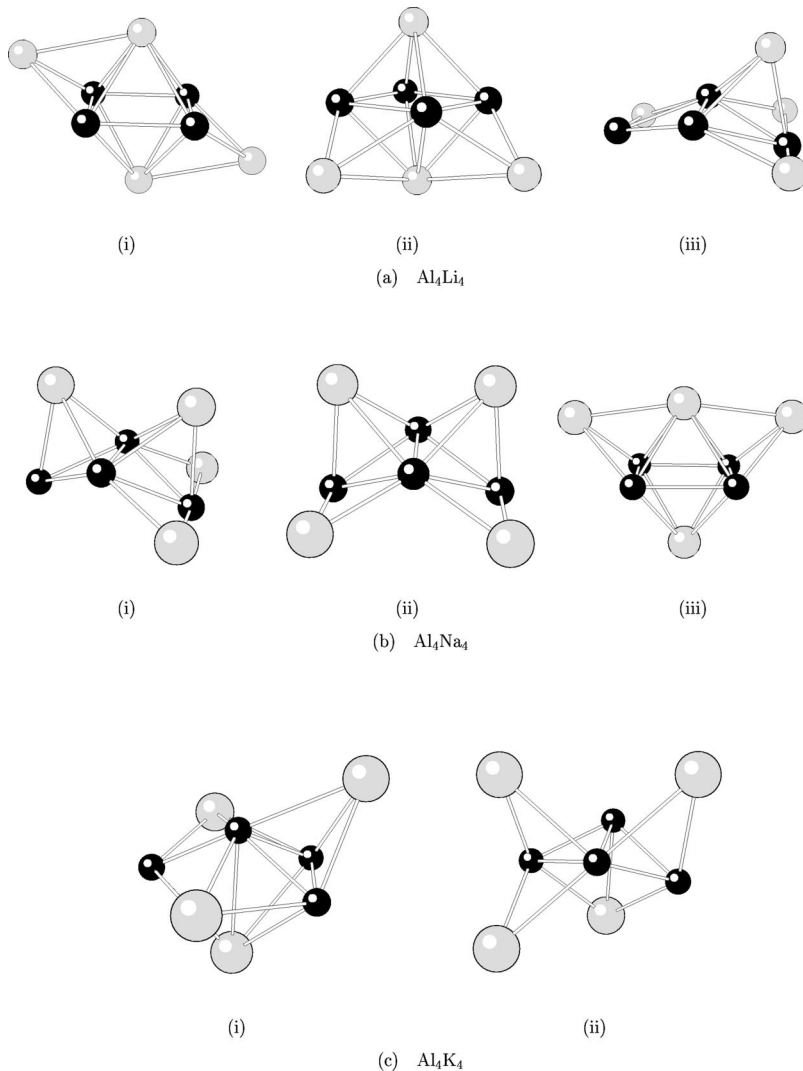


FIG. 1. The lowest energy state and the low-lying geometries of Al_4X_4 ($X=\text{Li}, \text{Na}, \text{K}$) clusters. Black circle represents Al atoms and shaded one represent X atoms. Figures captioned as (i) represent the lowest energy structure.

II. COMPUTATIONAL DETAILS

We have used BOMD based on Kohn–Sham formulation of density-functional theory using the damped Joannopoulos³⁹ method to obtain the low-energy structures of Al_4X_4 . This has permitted us to use a fairly moderate time step ≈ 80 a.u. The geometries of the clusters have been obtained by starting with different configurations like cubic, capped tetrahedron, bicapped trigonal prism, etc. The clusters were heated to 600–800 K and in certain cases up to 1800 K, followed by slow cooling. In all the cases, the stability of lowest energy configuration has been tested by reheating the cluster with a different geometry. Some additional structures were obtained by steepest-descent method starting from a suitable configuration during the simulated annealing run. Many of the low-energy structures have been verified by interchanging the positions of Al and X atoms and repeating the calculations. In general, we find that there are many isomeric structures nearly degenerate to the lowest energy state, quite a few of which were obtained by interchanging Al and X atoms or by rearranging the capping positions of one type of atoms. We have used the norm-conserving pseudopotential of Bachelet⁴⁰ *et al.* in Kleinman and Bylander⁴¹ form with s part treated as nonlocal. The

exchange-correlation potential was calculated using the local-density approximation (LDA) due to Barth and Hedin.⁴² A cubic supercell of length 40 a.u. with an energy cutoff of ≈ 11 Ry was found to provide sufficient convergence of the total energy. During the dynamics, the norm of each of the states defined as $|\langle h\psi_i - \epsilon_i\psi_i |^2$ (ϵ_i being an eigenvalue corresponding to eigenstate ψ_i of the Hamiltonian h) was maintained at 10^{-4} – 10^{-6} a.u. The structures were considered to be converged when the forces on all atoms were less than 10^{-4} a.u.

III. RESULTS AND DISCUSSION

In this section we discuss the low-energy structures, the energetics, and the bonding trend in Al_4X_4 clusters. First we discuss the evolution of their geometries. The geometries of the alkali-based clusters and those of the remaining clusters are shown in Figs. 1 and 2, respectively. The lowest energy structure of Al_4Li_4 [Fig. 1(a)(i)] is a capped octahedron with four Al atoms forming a rhombus, while the low-energy geometry [Fig. 1(a)(ii)] differs from it in the capping positions of Li. In another structure [Fig. 1(a)(iii)] Al is seen to form a quinted roof. Upon substitution of Li by Na, the planar struc-

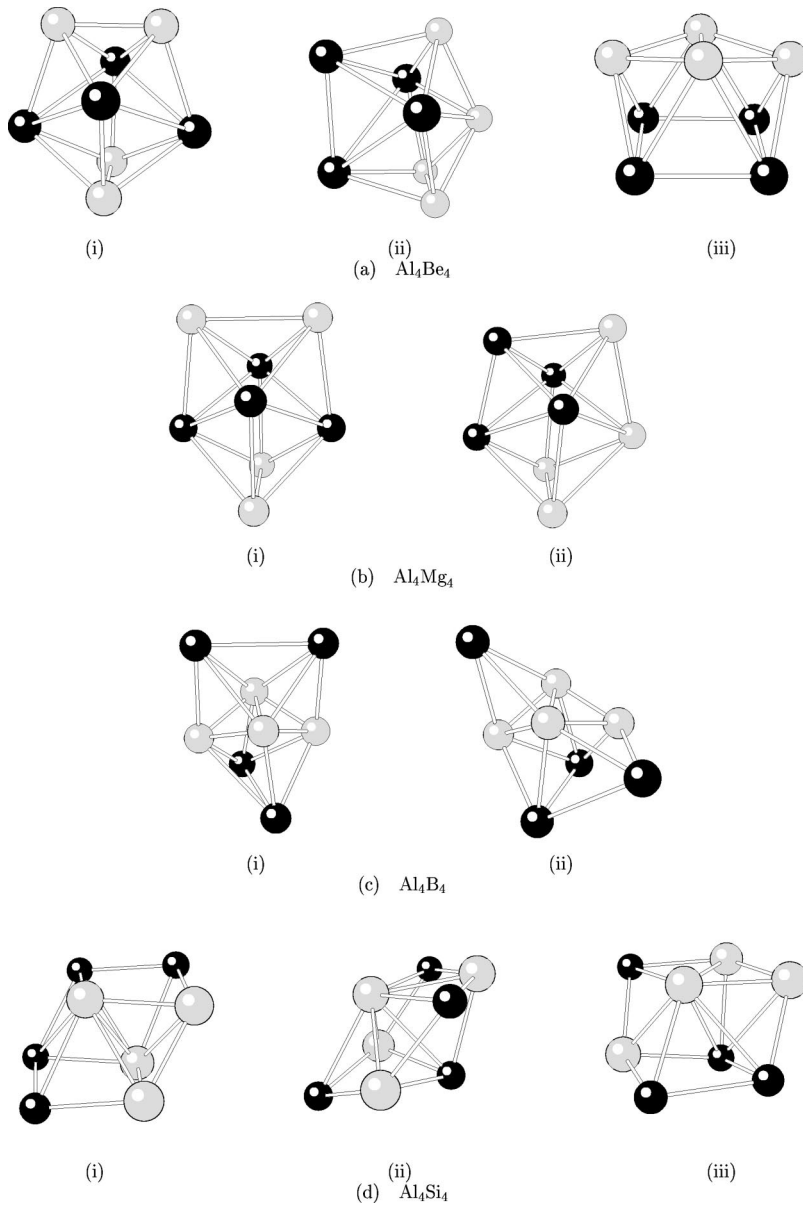


FIG. 2. The lowest energy state and the low-lying geometries of Al_4X_4 ($X = \text{Be}, \text{Mg}, \text{B}, \text{Si}$) clusters. Black circle represents Al atoms and shaded one represent X atoms. Figures captioned as (i) represent the lowest energy structure.

ture of Al_4 gets distorted to form a quinted roof [Fig. 1(b)(i)] which is nearly degenerate to the structure shown in Fig. 1(b)(ii). A capped octahedron [Fig. 1(b)(iii)] is one of its low-lying state. Substitution of Na by K having a larger ionic radius (1.33 Å) than Na (0.97 Å) (Ref. 43) further buckles the quinted roof of Al forming a pentagonal ring of three Al and two K leading to a capped pentagonal bipyramid [Fig. 1(c)(i)]. The capped quinted rooflike structure shown in Fig. 1(c)(ii), is seen to be the low-energy state. Thus it can be seen that the alkali-metal elements progressively distort the Al_4 structure upon formation of Al_4X_4 system. It may be recalled that the ground-state structure of Al_4 is rhombus.^{12,30} The lowest energy structure of both Al_4Be_4 and Al_4Mg_4 are similar in the sense that they can be described as a capped quinted roof, whereas their low-lying structures [Figs. 2(a)(ii) and 2(b)(ii)] are formed by interchanging one Al with Be and Mg, respectively. Al_4Be_4 also exhibits an Archimedean antiprism as one of its excited state structure [Fig. 2(a)(iii)]. Figure 2(b)(i) can also be viewed as

an Archimedean antiprism formed by a pair Al and Mg. In Al_4B_4 , the quinted roof structure seen in Al_4Mg_4 is maintained with the inner core of aluminum replaced by boron [Fig. 2(c)(i)]. The low-lying structure [Fig. 2(c)(ii)] can be obtained by rearranging the capping positions of Al. The geometries of Al_4Si_4 are quite different from the ones above. They can be viewed as capped heptamers of Al_8 (Refs. 12 and 30) with four sites of Al substituted by Si [Fig. 2(d)(i)]. We have repeated the geometry optimization for Al_4Na_4 and Al_4Si_4 clusters using generalized gradient approximation (GGA).⁴⁴ It was found that there is a reversal of the order with respect to the LDA geometries. However, the energy differences after reordering were less than 0.02 eV. Hence the binding-energy trend in Al_4X_4 clusters is not affected by GGA. Such reversal in geometries of mixed Al-Na clusters having an energy difference of the order of 0.1 eV have been observed by Dhavale *et al.*³³

Now we discuss the trend in binding energies in these clusters. The binding energy per atom of Al_4X_4 clusters, de-

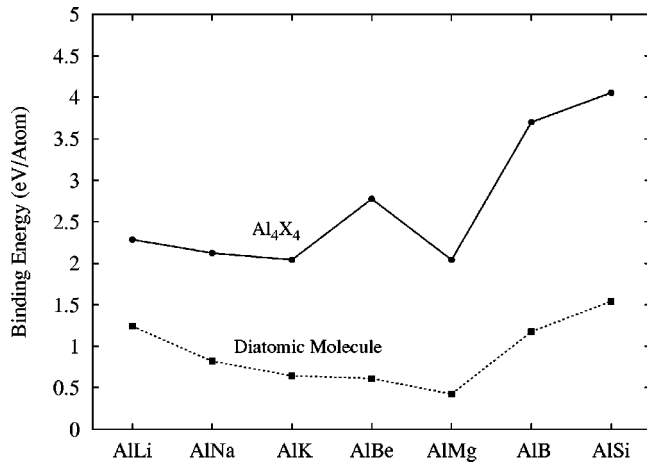


FIG. 3. The binding energy per atom of the diatomic molecules AlX (dotted lines) and the Al₄X₄ clusters (continuous line).

defined as $E_b[\text{Al}_4\text{X}_4] = -\frac{1}{8}(E[\text{Al}_4\text{X}_4] - 4E[\text{Al}] - 4E[\text{X}])$, and that of corresponding diatomic molecules AlX is plotted in Fig. 3. The trend in binding energies of diatomic molecules AlX and that of the corresponding Al₄X₄ clusters is similar with the exception of Al₄Be₄. A substantial rise in the binding energy in Al-Be system is seen in going from diatomic molecule to Al₄X₄ cluster. This rise in binding energy is due to the strongly bonded beryllium and is consistent with the observations by Kawai *et al.*⁴⁵ They showed that the behavior of Be clusters approaches the bulk very quickly as the function of cluster size. The binding energies of the alkali-metal-based Al₄X₄ clusters are nearly the same. The high binding energy of Al₄B₄ and Al₄Si₄ clusters is mainly due to the strong localized bond between B-B and Si-Si, respectively.

The nature of bonding in some Al-Li clusters, viz. Al₁₃Li, Al₁₂Li₄, Al₁₁Li₇, and Al₁₀Li₈, has been discussed by Kumar.³⁵ These clusters are found to have ionic bond between Li atoms and the strongly electronegative Al superatom. A similar charge transfer in Al-Li clusters has also been observed by Landman *et al.*¹⁸ In order to examine the validity of such behavior of Al₄ in Al₄X₄ clusters (X=Li, Na, K), we show, in Fig. 4, the difference charge density $\Delta\rho$, defined as $\Delta\rho = \rho_{\text{scf}} - \rho_{\text{superimpose}}$, where ρ_{scf} is the self-consistent total charge density and $\rho_{\text{superimpose}}$ is the overlapped atomic charge densities of the constituent atoms. The left-hand panel shows the charge depletion region and the right-hand panel shows the excess charge region. Quite clearly there is a charge transfer from the alkali-metal atoms to the Al₄ cluster, the bonding between them being ionic. It may be mentioned that Al₄ cluster is known to have a higher electron affinity of 2.20 eV (Ref. 31) than that of the alkali-metal atoms (Li: 0.62 eV; Na: 0.55 eV; K: 0.45 eV).⁴⁶ Thus, in these clusters, the four Al behaves as single entity or superatom and follows the electronic shell-filling-like atoms. It is interesting to compare the eigenvalue spectrum of these clusters and that of the free Al₄ having the same geometry as in Al₄X₄ cluster. Figure 5 shows such an eigenvalue plot. The spectrum of Al₄X₄ clusters has been lowered so that its lowest eigenvalue coincides with that of the Al₄. Evidently,

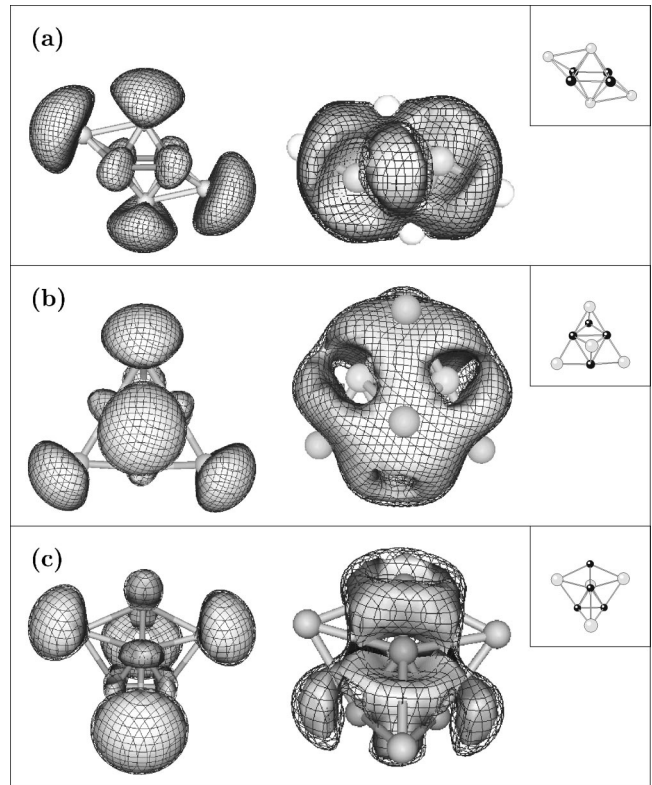


FIG. 4. Difference charge-density ($\Delta\rho$) surfaces for (a) Al₄Li₄, (b) Al₄Na₄, and (c) Al₄K₄. The left-hand panel is the charge depleted region and the right-hand panel is the charge excess region. The orientation of the cluster is shown in the inset. The values of the charge densities are 0.000 63, 0.000 81, 0.0060 electrons/a.u.³ for the left-hand panel and 0.0012, 0.001 04, 0.0023 electrons/a.u.³ for the right-hand panel, respectively.

the first four eigenvalues of Al₄ do not change upon formation of Al₄X₄ cluster clearly indicating its superatom behavior. This may be taken as an indication of monovalent nature of Al in small clusters. Further, the examination of the char-

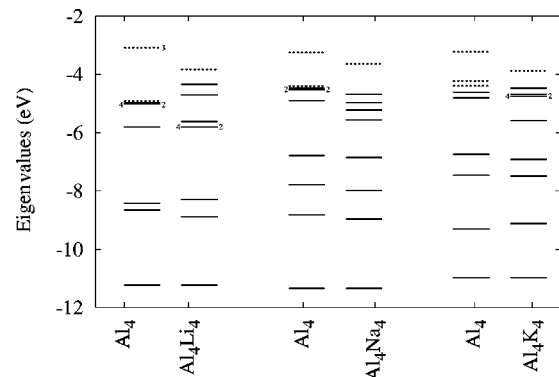


FIG. 5. The eigenvalue spectrum of Al₄X₄ (X=Li, Na, K) clusters and Al₄ having the same geometry as in Al₄X₄. Continuous lines represent occupied eigenstates and dotted ones represent unoccupied eigenstates. Whenever the levels are degenerate or closely spaced, the total number of levels in that bunch is indicated by the number at right. The numbers on the left indicate the total number of electrons occupied by that bunch.

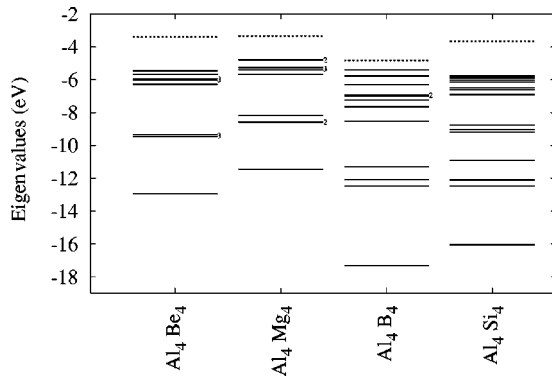


FIG. 6. The eigenvalue spectrum of Al_4X_4 ($X=\text{Be}, \text{Mg}, \text{B}, \text{Si}$) clusters. The continuous lines represents occupied eigenstates and the dotted one represents LUMO eigenstates. Whenever the levels are degenerate or closely spaced, the total number of levels is indicated by the number at right.

acter of the eigenstates of these clusters indicate that they are consistent with the jellium description.

The eigenvalue spectrum of the remaining clusters, shown in Fig. 6, indicates a jellium behavior for the 20 valence electron systems Al_4Be_4 and Al_4Mg_4 . Further, both spectra show a large HOMO-LUMO gap of 2.07 and 1.47 eV, respectively, as compared to that of the alkali counterpart 0.52, 1.05, and 0.66 eV, respectively, which is expected due to the shell closing effect. Here Al displays a trivalent character. There is no signature of superatom in these clusters in the sense that it is not possible to identify the core levels belonging to any one type of atom. In addition, the total charge density (not shown) was found to be completely delocalized throughout the cluster.

The eigenvalue spectrum for Al_4B_4 and Al_4Si_4 clusters are nonjellium, i.e., their character cannot be classified as pure s, p, d, \dots type. The bonding in these clusters can be explained by examining the isodensity plots of the total charge density shown in Fig. 7. A localized charge distribution along B-B and Si-Si is clearly evident. Interestingly, the behavior of the Al-Al bond is similar to that of Si-Si, i.e., localized. A depletion of charge around Al is also seen. This is consistent with the fact that Al has three-valence electron and is tetrahedrally bonded with other Al and Si atoms. The behavior of Al and Si in this cluster can be contrasted with that of a single Si in Al_n clusters where the behavior of Si is free-electron-like.⁴⁷ In case of Al_4B_4 clusters, a similar localized charge distribution can be seen along the shorter Al-Al bond which is also closer to the boron atoms.¹³

Finally, we compare the behavior of Na and K in Al_4X_4 cluster in the light of the fact that these two elements are completely immiscible with Al in bulk phase.³⁶ Their solubility is very low in liquid phase. In order to discuss this behavior we have plotted, in Fig. 8, the minimum interatomic separations Al-Al, Al-X, and X-X for all the clusters. The ionic radii of Na and K are larger than Al. It can be seen immediately that Al-K and K-K bonds are much larger than the Al-Al. On the other hand, in Al_4Na_4 cluster, though Na-Na bond is rather large, the Al-Al and Al-Na bond distances are of the same order. Also, the nearest-neighbor dis-

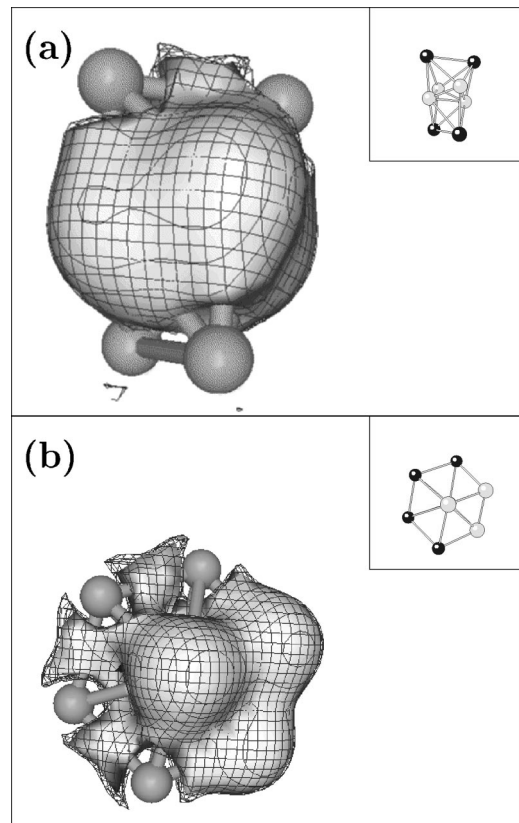


FIG. 7. Constant charge-density surfaces of the total charge density for (a) Al_4B_4 and (b) Al_4Si_4 . The orientation of the cluster is shown in the inset. The charge densities have been given for 0.032, 0.035 electrons/a.u.³, respectively.

tances for the remaining clusters are of the same order. Thus even in small clusters the tendency for K not to mix with Al shows up whereas for Na it is not seen. Evidently, this can be attributed to rather large differences between the ionic radii of Al and K.

IV. CONCLUSION

In the present work, we have reported the geometries and the systematics of bonding in a series of Al_4X_4 ($X=\text{Li}, \text{Na}$,

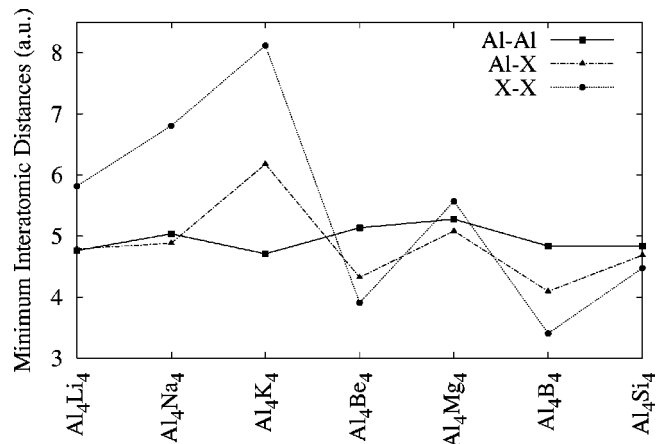


FIG. 8. The minimum interatomic separations Al-Al (continuous line), Al-X (dashed line), and X-X (dotted line) in Al_4X_4 clusters.

K, Be, Mg, B, and Si) clusters using BOMD method within the framework of density-functional theory. All the clusters with metallic elements were found to conform the SJM. The 20 valence electron systems Al_4Be_4 and Al_4Mg_4 shows a significant HOMO-LUMO gap. In clusters containing alkali-metal atoms, Al_4 behaves as a superatom and is ionically bonded to them. The Al-Al bond in Al_4Si_4 and Al_4B_4 clusters is found to be covalent indicating that Al with valency three behaves like Si in these systems. Even in small clusters the immiscibility of K shows up.

ACKNOWLEDGMENTS

We gratefully acknowledge the partial financial assistance from Indo-French Center for the Promotion of Advanced Research (New Delhi)/Center Franco-Indian Pour la Promotion de la Recherche Avancée. M.D. acknowledges the University Grants Commission, India, and S.C. gratefully acknowledges financial support from CSIR (New Delhi). It is a pleasure to acknowledge Professor S. R. Gadre for the use of graphics software Univis 2000.

*Email address: chacko@physics.unipune.ernet.in

†Email address: mdd@physics.unipune.ernet.in

‡Email address: kanhere@physics.unipune.ernet.in

¹Vijay Kumar, K. Esfarjini, and Y. Kawazoe, *Advances in Cluster Science* (Springer-Verlag, Heidelberg, 2000).

²J. Chang, M. J. Stott, and J. A. Alonso, *J. Chem. Phys.* **104**, 8403 (1996); P. R. Schleyer and J. Kapp, *Chem. Phys. Lett.* **255**, 363 (1996); C. Marsden, *ibid.* **245**, 475 (1995); K. Albert, K. M. Neyman, V. A. Nasluzov, S. Ph. Ruzankin, Ch. Yeretizian, and N. Rösh, *ibid.* **245**, 671 (1995).

³*Clusters and Nanostructured Materials*, edited by P. Jena and S. N. Behera (Nova Science Publishers, Inc., New York, 1996).

⁴C. Yeretizian, U. Rothlisberger, and E. Schumacher, *Chem. Phys. Lett.* **237**, 334 (1995).

⁵R. O. Jones, A. I. Lichtenstein, and J. Hutter, *J. Chem. Phys.* **106**, 4566 (1997).

⁶I. Boustani, W. Pewestorf, P. Fantucci, V. Bonačić-Koutecký, and J. Koutecký, *Phys. Rev. B* **35**, 9437 (1987).

⁷Ursula Röthlisberger and Wanda Andreoni, *J. Chem. Phys.* **94**, 8129 (1991).

⁸F. Spiegelmann and D. Pavolini, *J. Chem. Phys.* **89**, 4954 (1988).

⁹Zhi-Xiong Cai, S. D. Mahanti, A. Antonelli, S. N. Khanna, and P. Jena, *Phys. Rev. B* **46**, 7841 (1992).

¹⁰V. Kumar and R. Car, *Phys. Rev. B* **44**, 8243 (1991).

¹¹Vlasta Bonačić-Koutecký, Piercarlo Fantucci, and Jaroslav Koutecký, *Chem. Rev.* **91**, 1035 (1991).

¹²R. O. Jones, *J. Chem. Phys.* **99**, 1194 (1993).

¹³Ihsan Boustani, *Chem. Phys. Lett.* **233**, 273 (1995); Ihsan Boustani, *Phys. Rev. B* **55**, 16 426 (1997).

¹⁴Xiaodun Jing, N. Troullier, David Dean, N. Binggeli, James R. Chelikowsky, K. Wu, and Y. Sadd, *Phys. Rev. B* **50**, 12 234 (1994).

¹⁵Vijay Kumar, in *Proceedings of the 8th National Workshop on Atomic and Molecular Physics*, edited by A. P. Pathak (Nova Publications, Narosa, 1990).

¹⁶Gianfranco Pacchioni and Jaroslav Koutecký, *Chem. Phys.* **71**, 181 (1982).

¹⁷W. D. Knight, K. Clemenger, W. A. de Heer, W. A. Saunders, M. Y. Chou, and M. L. Cohen, *Phys. Rev. Lett.* **52**, 2141 (1984).

¹⁸Hai-Ping Cheng, R. N. Barnett, and Uzi Landman, *Phys. Rev. B* **48**, 1820 (1993).

¹⁹P. Fantucci, V. Bonačić-Koutecký, W. Pewestorf, and J. Koutecký, *J. Chem. Phys.* **91**, 4229 (1989).

²⁰W. Pewestorf, V. Bonačić-Koutecký, and J. Koutecký, *J. Chem. Phys.* **89**, 5794 (1988).

²¹Ajeeta Dhavale, Vaishali Shah, and D. G. Kanhere, *Phys. Rev. A*

57, 4522 (1998).

²²Ajeeta Dhavale, D. G. Kanhere, C. Majumdar, and G. P. Das, *Eur. Phys. J. D* **6**, 495 (1999).

²³M. Deshpande, A. Dhavale, R. R. Zope, S. Chacko, and D. G. Kanhere, *Phys. Rev. A* **62**, 063202 (2000).

²⁴P. Ballone, W. Andreoni, R. Car, and M. Parrinello, *Europhys. Lett.* **8**, 73 (1989).

²⁵A. Bol, J. A. Alonso, and J. M. Lopez, *Int. J. Quantum Chem.* **56**, 839 (1995).

²⁶J. A. Alonso, *Phys. Scr.* **T55**, 177 (1994).

²⁷C. Majumdar, S. K. Kulshreshtha, G. P. Das, and D. G. Kanhere, *Chem. Phys. Lett.* **311**, 62 (1999).

²⁸A. M. Al-Laham and K. Raghavachari, *J. Chem. Phys.* **98**, 8770 (1993).

²⁹J. A. Alonso, L. M. Molina, M. J. Lopez, A. Rubio, and M. J. Stott, *Chem. Phys. Lett.* **289**, 451 (1998).

³⁰B. K. Rao and P. Jena, *J. Chem. Phys.* **111**, 1890 (1999).

³¹B. K. Rao and P. Jena, *J. Chem. Phys.* **113**, 1508 (2000).

³²F. Duque and A. Mananes, *Eur. Phys. J. D* **9**, 223 (1999).

³³Ajeeta Dhavale, D. G. Kanhere, S. A. Blundell, and R. Zope (unpublished).

³⁴B. K. Rao, S. N. Khanna, and P. Jena, *Phys. Rev. B* **62**, 4666 (2000).

³⁵Vijay Kumar, *Phys. Rev. B* **60**, 2916 (1999).

³⁶A. R. Bailey, *A Text-Book of Metallurgy*, 2nd ed. (Macmillan Student Editions, New York, 1967).

³⁷S. N. Khanna and P. Jena, *Chem. Phys. Lett.* **219**, 479 (1994).

³⁸M. C. Payne, M. P. Teter, D. C. Allan, T. A. Arias, and J. D. Joannopoulos, *Rev. Mod. Phys.* **64**, 1045 (1992).

³⁹D. C. Payne and J. D. Joannopoulos, *Phys. Rev. Lett.* **56**, 2656 (1986).

⁴⁰G. B. Bachelet, D. R. Hamann, and M. Schluter, *Phys. Rev. B* **26**, 4199 (1982).

⁴¹L. Kleinman and D. M. Bylander, *Phys. Rev. Lett.* **48**, 1425 (1982).

⁴²U. Barth and L. Hedin, *J. Phys. C* **5**, 1629 (1972).

⁴³Charles Kittel, *Introduction to Solid State Physics*, 7th ed. (John Wiley & Sons, Inc., New York, 1995).

⁴⁴J. P. Perdew, K. Burke, and M. Ernzerhof, *Phys. Rev. Lett.* **77**, 3865 (1996).

⁴⁵R. Kawai and J. H. Weare, *Phys. Rev. Lett.* **65**, 80 (1990).

⁴⁶*CRC Handbook of Chemistry and Physics*, edited by David R. Lide, 74th ed. (CRC, Boca Raton, Florida, 1993–1994).

⁴⁷Vijay Kumar and V. Sundarajan, *Phys. Rev. B* **57**, 4939 (1998); Vijay Kumar, Satadeep Bhattacharjee, and Yoshiyuki Kawazoe, *ibid.* **61**, 8541 (2000).